



LncRNA PCIF1 promotes aerobic glycolysis in A549/DDP cells by competitively binding miR-326 to regulate PKM expression

Wan Zhong^c, Chun Wang^{b,**}, Ye Sun^{a,*}

^a Department of Pathogenic Biology, Shenyang Medical College, 146 Huanghe North Street, Yuhong District, Shenyang, 110034, China

^b Department of Cell Biology, College of Integrated Chinese and Western Medical, Liaoning University of Traditional Chinese Medicine, 79 Chongshan Eastern Road, Huang gu District, Shenyang, 110847, China

^c Department of Obstetrics and Gynecology, General Hospital of the Northern Theater Command, 83 Wenhua Road, Shenhe District, Shenyang, 110016, China

ARTICLE INFO

Keywords:

NSCLC
Cisplatin-resistant
Glycolysis
Lnc-PCIF1
PKM

ABSTRACT

Objective: Utilizing transcriptome analysis to investigate the mechanisms and therapeutic approaches for cisplatin resistance in non-small cell lung cancer (NSCLC).

Methods: Firstly, the biological characters of A549 cells and A549/DDP cells were detected by RNA sequencing, CCK-8 and hippocampal energy analyzer. Then, the differential Genes were functionally enriched by GO and KEGG and the competitive endogenous RNA network map was constructed. Finally, the effects of the predicted biogenesis pathway on the biological functions of A549/DDP cells were verified by in vitro and in vivo experiments.

Result: The differentially transcribed genes of A549 and A549/DDP cells were analyzed by enrichment analysis and cell biological characteristics detection. The results showed that A549/DDP cells showed significantly increased resistance to cisplatin, glucose metabolism signaling pathway and glycolysis levels compared with A549 cells. Among glycolysis-related transcription genes, PKM had the most significant difference Fold Change is 8. LncRNA PCIF1 is a new marker of A549/DDP cells and can be used as a molecular sponge to regulate the expression of PKM. LncRNA PCIF1 targets miR-326 to induce PKM expression, promote glycolysis level, and enhance the resistance of A549/DDP cells to cisplatin.

Conclusion: LncRNA PCIF1 as biomarkers of A549/DDP cells, higher expression can induce the PKM, promote cell glycolysis, lead to the occurrence of cisplatin resistance. LncRNA PCIF1 can be considered as a potential target for treating cisplatin-resistant NSCLC.

1. Introduction

Studies have found that less than 10 % of human genome sequences are transcribed into RNA, and the vast majority are non-coding RNAs (ncRNAs), which regulate life activities, affecting embryonic development, metabolism, and tumorigenesis [1]. During the past two decades, research on microRNAs (miRNAs) has trended deeper and extensive, and it has been found that they can degrade by combining with messenger RNAs (mRNAs) to regulate the opening or closing of genes [2], especially in the field of oncology. In recent years, studies have confirmed the equal importance of long ncRNAs (lncRNAs) in regulating gene expression, which act by indirectly affecting mRNA expression through complementary pairings with miRNAs. Until now, nearly 20,

000 lncRNAs have been identified, but only a small portion can clarify the regulatory mechanism, and there are still many unknown biological functions of lncRNAs to be explored [3,4]. Although the regulatory mechanisms of lncRNAs have not been clearly studied, it can be believed that they act at multiple levels, such as DNA replication, mRNA transcription, and protein translation, directly or indirectly affecting the development, deterioration, and drug resistance of tumors [5–8].

The number of deaths annually from lung cancer worldwide is close to 1 million, ranking it first among all malignant tumors [9]. Eighty percent of patients have entered an advanced stage of lung cancer at the time of diagnosis and lost the opportunity for surgical treatment [10]. Currently, platinum-based chemotherapy is mainly used in clinical treatment for anti-tumor purposes [11], but the frequency of drug

* Corresponding author.

** Corresponding author.

E-mail addresses: 1205055348@qq.com (C. Wang), sunye@symc.edu.cn (Y. Sun).

<https://doi.org/10.1016/j.mcp.2024.101977>

Received 7 July 2024; Received in revised form 20 July 2024; Accepted 27 July 2024

Available online 7 August 2024

0890-8508/© 2024 The Authors. Published by Elsevier Ltd. This is an open access article under the CC BY license (<http://creativecommons.org/licenses/by/4.0/>).

resistance of tumors is increasing. In recent years, studies have confirmed that tumor cells meet their growth and metabolic needs through aerobic glycolysis. Tumor cells by glycolysis rapidly produce ATP and some enzymes and metabolic product of glycolytic pathway to promote the growth and proliferation of tumor cells, invasion and metastasis, antiapoptotic effect, develop resistance to chemotherapy drugs [12–14]. Pyruvate Kinase, including PKM1 and PKM2, is a key enzyme in the glycolytic pathway. A large number of literatures have confirmed that PKM is closely related to the occurrence and development of a variety of tumors [15,16]. PKM by participating in the glycolysis process and interact with other biological molecules, affect the NSCLC cell proliferation, migration and resistance, which is closely related to the progress of NSCLC [17].

In this study, Cisplatin-resistant human lung adenocarcinoma cell line A549/DDP and its parent A549 cell line were selected as model cell lines. The differences in gene expression and glycolysis of A549/DDP cells were analyzed by RNA-Seq technology and cellular energy metabolism analyzer. By constructing the ceRNA regulatory network, we explored the molecular mechanism of how lncRNA induces cisplatin resistance in A549/DDP cells by regulating the level of cellular glycolysis. The experimental results of this study lay a theoretical foundation for more effective treatment of lung adenocarcinoma in the future.

2. Materials and methods

2.1. Cell lines and cell culture

A549 cells were procured from Beijing Dingguo Changsheng Biotechnology Co., Ltd. The biologically stable strains were cultured in vitro for the purpose of conducting studies related to non-small cell lung cancer (NSCLC). A549/DDP human lung adenocarcinoma cells were procured from Beijing Xiehe Cell Resource Center and cultured with cisplatin in vitro to establish biologically stable strains for NSCLC-related studies. Both A549 and A549/DDP cells were cultured in Dulbecco's modified Eagle's medium (DMEM)/high glucose (Hyclone Laboratories, Logan, UT, USA) containing 10 % fetal bovine serum (Hyclone Laboratories, Logan, UT, USA) at 37 °C, 95 % humidity, and 5 % CO₂. Cell growth was observed regularly. Cell passage could be carried out with a growth density of 80–90 %. To maintain the good cisplatin-resistance stability of A549/DDP cells, they were continuously cultured in a low-concentration cisplatin environment (7 μM) (Sigma-Aldrich, St. Louis, MO, USA). The cisplatin was removed two weeks before the experiment.

2.2. Reagents and antibodies

Cisplatin is purchased from Sigma (MO, USA). Antibodies include rabbit PKM polyclonal antibody, rabbit BAX polyclonal antibody, mouse capase 3/p17/p19 polyclonal antibody, mouse Bcl2 monoclonal antibody, goat anti-mouse IgG and goat anti-rabbit IgG purchased from Proteintech (Wuhan, China).

2.3. RNA-seq data acquisition

Total RNA was extracted by TRIzol solution, and RNA content and integrity were detected by NanoDrop ND-1000 and agarose gel electrophoresis. NEB Next®Poly (A) mRNA Magnetic Separation Module kit (New England Biolabs, Ipswich, MA, USA) and KAPA strand RNA-seq library Preparation kit (Illumina, San Diego, CA, USA) were used for mRNA enrichment and library construction, and the amplified fragments were sequenced by Illumina sequencer.

2.4. RNA-seq data analysis

The original FASTQ sequences generated by Illumina sequencers meet Q30 ≥ 80 % and FPKM >0.5, which can be used for subsequent

statistical analysis. By conducting a PCA of genes with significant differences in mean (analysis of variance [ANOVA]) values between samples ($P < 0.05$) to show the classification of data, we can obtain the intuitive distribution of samples between the experimental group and the control group, detect and remove outliers, and find out the sample set with high similarity.

2.5. GO and KEGG enrichment analysis

GO enrichment analysis used Fisher's exact test to identify specific functional items that were most closely related to differentially expressed genes, and each GO item corresponded to a statistical value (P-value), indicating significance. KEGG pathway enrichment analysis method mainly matches the differentially expressed mRNA between samples with the biological pathway resource entries in the KEGG database, then compares and enriches these differentially expressed mRNA with known functional entries, and finally gets a set of relationship graphs between differentially expressed genes and specific functional entries.

2.6. Construction of the competing endogenous (ceRNA) network

The molecular mechanism of ceRNA can be summarized as follows: endogenous lncRNAs regulate the activity of miRNAs by combining with them, thereby affecting the interaction between miRNAs and mRNAs and finally causing changes in gene expression. To find the potential miRNA targets, TargetScan and miRNA software are usually used to predict them. The ceRNA network was constructed by summarizing common miRNAs.

2.7. Cell inhibition test of cisplatin

The number of cells per well was 5×10^3 . A549 cells and A549/DDP cells in the logarithmic phase of growth were inoculated on 96-well plates and adhered to the wall overnight. We removed the culture medium the next day, added cisplatin (12, 24, 48, 96, or 192 μM) to the DMEM culture medium, intervened cells for 24 h, and added 10 μL of cell counting kit 8 solution. After incubation at 37 °C for 4 h, the absorbance value was detected under the absorbance wavelength of 460 nm. Each group of experiments was repeated three times.

2.8. Cell glycolysis pressure measurement

The dynamic changes of glycolysis level in A549 cells and A549/DDP cells during growth were detected by Seahorse XF glycolytic stress test. We inoculated 8×10^3 A549 and A549/DDP cells onto a Seahorse XF microplate and then incubated the plate in a CO₂-free incubator at 37 °C for 24 h. After removing the cell culture microplate from the incubator, we changed the cell growth medium into a warm detection solution and then placed the cell culture microplate into a 37 °C CO₂-free incubator for 1 h. Subsequently, we ran the Seahorse XF glycolysis pressure test and data analysis.

2.9. Glucose consumption and lactate production assay

We added an 80–90 % density of A549 cells and A549/DDP cells into the lysate with reference to the instructions of the reagent and fully lysed the cells by vortex vibration. The culture medium and cells were collected separately, and glucose concentration and lactate production were measured using the Glucose assay kit (Applygen, Beijing, China) and the Lactic Acid assay (Jiancheng Bioengineering Institute, Nanjing, China) in accordance with the manufacturers' protocols, and the glucose consumption level or the lactate production level was divided by the number of cells.

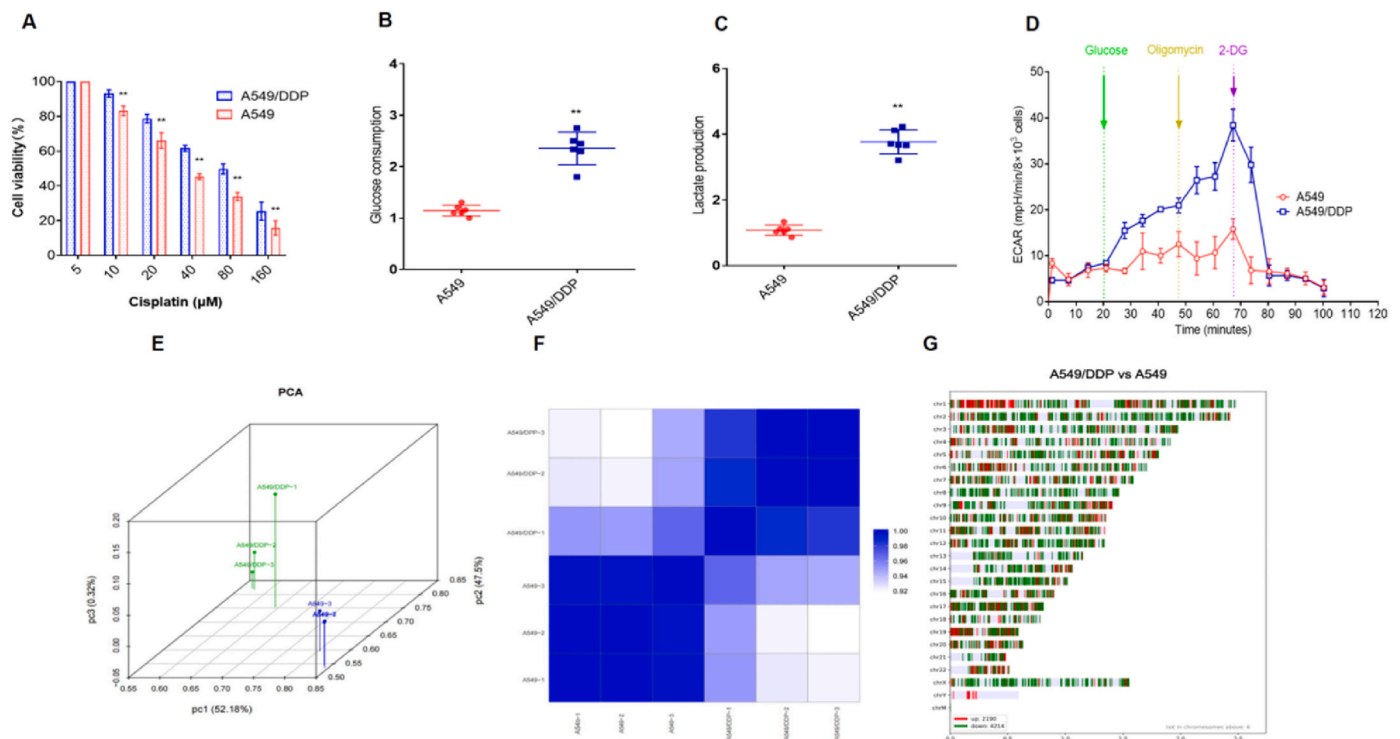


Fig. 1. Analysis of biological characters of A549/DDP cells and A549 cells. (A) The growth-inhibition effect of cisplatin on A549 cells and A549/DDP cells was determined. (B and C) Measurement of glucose consumption and lactic acid accumulation. (D) Determination of glycolysis pressure. (E) The intra- and inter-sample correlations were analyzed by principal component analysis; Each red dot represents a coding gene, and each blue dot represents a non-coding gene. (F) Matrix heat map method was used to analyze the correlation between samples and between samples. The deeper the color is, the higher the correlation. (G) Distribution of differential genes in chromosomes. The red dots represent upregulated differentially expressed genes, the green dots represent downregulated differentially expressed genes, and the grey dots represent the expression genes with no obvious differences. The experiments were repeated at least three times, and results were expressed as mean \pm S.D. *, $p < 0.05$; **, $p < 0.01$. (For interpretation of the references to color in this figure legend, the reader is referred to the Web version of this article.)

2.10. Synthesis of oligonucleotides and cell transfection

2×10^5 cells per well were injected into 6-well plates and cultivated overnight, with cell fusion reaching more than 70 %. GenePharma (Shanghai, China) synthesized miR-326 mimics and its miR-326 mimics NC or miR-326 inhibitor and its miR-326 inhibitor NC, which were then transfected into cells using the GoldenTran DR Reagent (Golden Trans Technology, Changchun, China) to achieve miR-326 overexpression or inhibition. The cDNA encoding PCIF1 was cloned into pcDNA3.1 vector and its control pcDNA3.1 empty vector or the knockout gene si-PCIF1 and its control si-NC were synthesized by GenePharma and transfected into cells to over-express or inhibit PCIF1 expression.

2.11. TUNEL assay

Cell climbs were first put on 24-well plates, followed by the seeding of 2×10^5 A549/DDP cells in each well. Following 16 h of adherent culture, cells from the control and drug experimental groups were introduced for 24 h. The slides were picked up with sterile forceps and cleaned with PBS once. The cells were fixed with 4 % paraformaldehyde for 30 min before being permeabilized with Triton X-100 solution (0.1 %) for 5 min at room temperature. 50 μ L of TUNEL detection solution was added and incubated at 37 $^{\circ}$ C in the dark for 60 min before being photographed using a fluorescence microscope.

2.12. EdU assay

A total of 5×10^4 cells were seeded into 24-well plates, and each experimental group and the blank control group were treated for 24 h according to the experimental requirements. After removing the culture medium and washing it twice with PBS, 200 μ L of $1 \times$ EdU solution at a

final concentration of 10 μ M was added and incubated for 2 h at room temperature. Cells were rinsed with PBS and fixed for 30 min in 4 % paraformaldehyde. Cells were stained with an EdU kit and DAPI staining solution (Beyotime Biotechnology, Shanghai, China). Images were captured with a Zeiss fluorescence microscope, and the number of cells stained with EdU and DAPI was counted with ImageJ software.

2.13. Luciferase assay

Wild-type or mutant PCIF1 or PKM was constructed into pmirGLO plasmids by GenePharma, miR-326 mimic or miR-NC, and Luciferase-reporter plasmids were transfected into HEK293 cells. Two substrates Luciferase were added 48 h later and luciferase activity was detected using a Dual-Luciferase Reporter Assay System.

2.14. Quantitative real-time PCR

RNA was extracted using RNA-easy Isolation Reagent (Vazyme, Shanghai, China). For miR-326, cDNA was produced using miRNA-specific reverse transcription primers, and qRT-PCR was carried out using the SYBR green dye technique with the Hairpin-itTM miRNA qRT-PCR Quantitation kit (GenePharma, Shanghai, China), as directed by the manufacturer. The following were the qRT-PCR conditions for miRNAs: 3 min at 95 $^{\circ}$ C, followed by 40 cycles of 12 s at 95 $^{\circ}$ C and 40 s at 62 $^{\circ}$ C. The expression of the U6 gene served as an internal control. For PCIF1 and PKM, and cDNA was reverse-transcribed using HiScript II Q Select RT SuperMix for qPCR Kit (Vazyme, Shanghai, China) at 37 $^{\circ}$ C for 15 min and 85 $^{\circ}$ C for 5 s. The target gene's expression was measured using the ChamQ Universal SYBR qPCR Master Mix (Vazyme, Shanghai, China) in triplicate under the following conditions: 95 $^{\circ}$ C for 30 s, followed by 40 cycles of 95 $^{\circ}$ C for 10 s and 60 $^{\circ}$ C for 30 s. The β -Actin gene

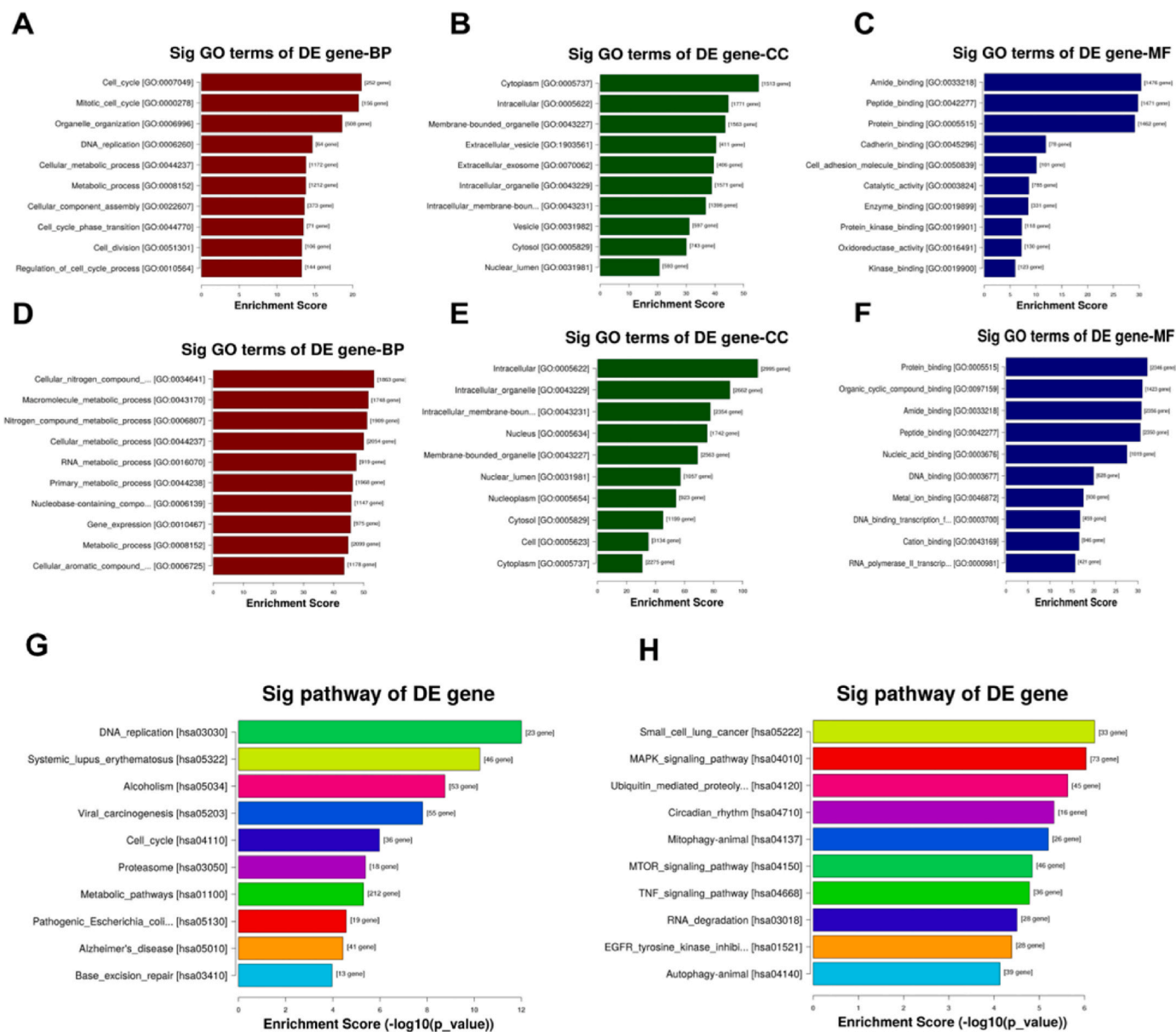


Fig. 2. Functional enrichment analysis of differential genes. GO analysis of differentially up-regulated genes, (A) Biological process, (B) cellular component, and (C) molecular function. GO analysis of differentially down-regulated genes, (D) Biological process, (E) cellular component, and (F) molecular function. KEGG enrichment map of differentially expressed genes, (G) upregulated and (H) downregulated genes.

was employed as an internal control. The relative mRNA expression was estimated using formula $2^{-\Delta\Delta Ct}$.

2.15. Western blot

A549 cells and A549/DDP cells, as well as A549/DDP cells after treatment in each experimental group, were lysed with RIPA solution to extract proteins. Equal quantities of protein samples from each group were added for SDS-PAGE electrophoresis at 80V 90 min. Protein bands from SDS-PAGE gel were transferred to PVDF membrane at 25V, 1.3A for 7 min. PVDF membranes containing proteins were washed with TBST before overnight blocking with 5 % skim milk, a 1-h incubation with primary antibody, and half a hour incubation with secondary antibody. Finally, the ECL solution was employed to create the imaging.

2.16. In vivo experiments

Female BALB/c nude mice were subcutaneously injected with 0.2 ml

of A549/DDP cells at a concentration of 1×10^7 cells/mL on the right side when the tumor had grown to 50–100 mm. The mice were then randomly divided into four groups (n = 5 in each group). The groups included si-NC + inhibitor-NC, si-PCIF1+inhibitor-NC, si-NC + inhibitor-miR-326, and si-PCIF1+inhibitor-miR-326. These combinations were injected into the tumors of the mice, and tumor size was observed after 7 days of intervention. Western blot analysis was used to detect protein expression levels.

2.17. Statistical analysis

The data are presented as mean \pm standard deviation values. During the statistical analysis of data, the difference between the two groups was analyzed using two-tailed Student's *t*-tests. ANOVA was used to analyze differences in multiple groups of data. *P* < 0.05 was chosen to indicate a statistically significant difference. SPSS software version 17.0 (IBM Corporation, Armonk, NY, USA) was used for statistical analysis.

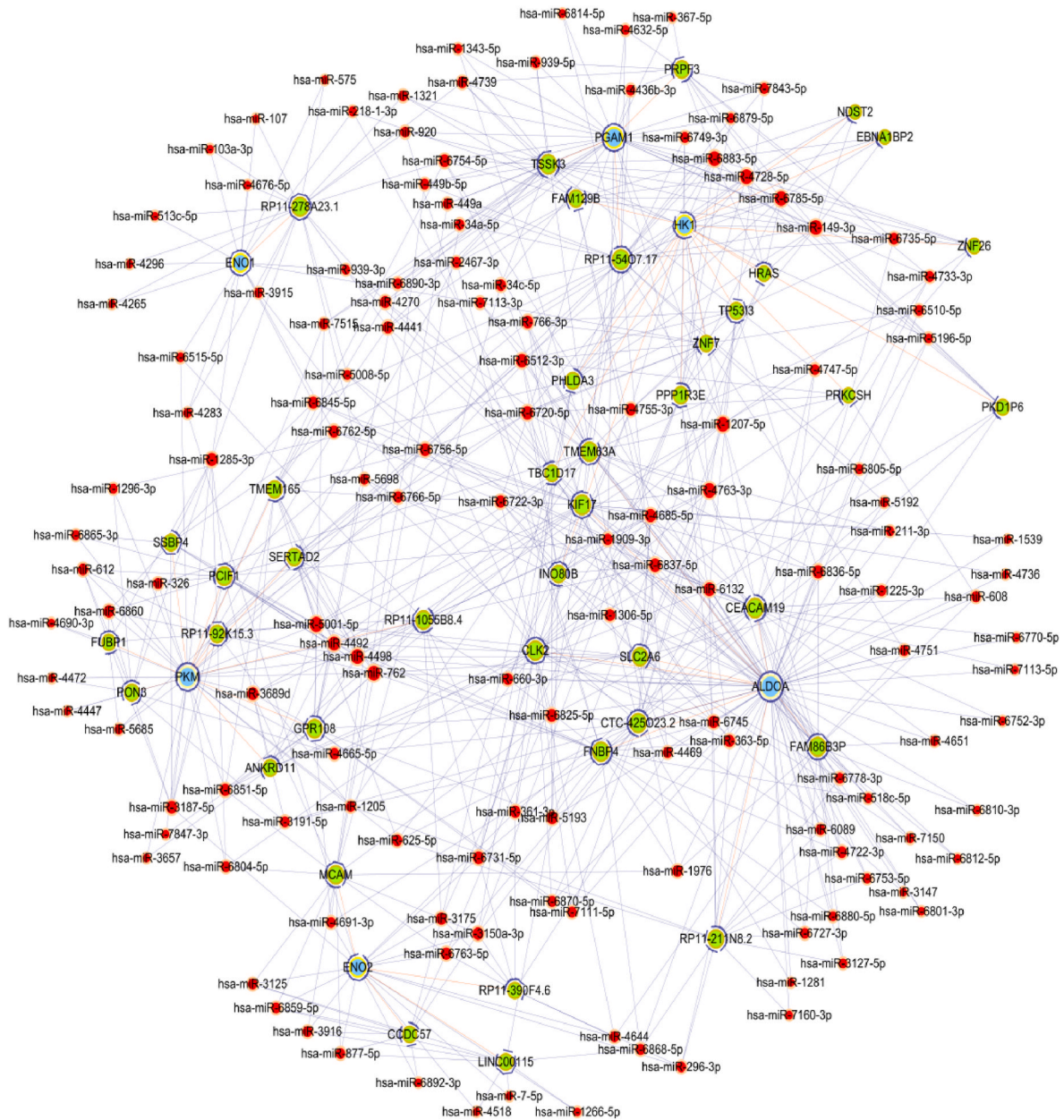


Fig. 3. Construction of the ceRNA network regulated by the glycolysis pathway.

3. Results

3.1. A549 cells and A549/DDP cell biological character difference analysis

As shown in Fig. 1-A, cisplatin can inhibit the viability of both A549 and A549/DDP cells in a concentration-dependent manner. A549/DDP cells have greater cisplatin resistance than A549 cells. The IC_{50} values of A549 and A549/DDP cells were 26.67 and 48 μ M, respectively. The glucose consumption and lactic acid accumulation of cisplatin-resistant A549/DDP cells were significantly increased compared to those of the parent A549 cells (Fig. 1-B and 1-C). In addition, the extracellular acidification rate was measured using a hippocampal cell energy meter and, as shown in Fig. 1-D, the extracellular acidification rate of A549/DDP cells was significantly higher than that of A549 cells.

As shown in Fig. 1-E and 2-F, PCA and heat map results showed a high correlation between three repeat samples of A549 cells and A549/DDP cells. Fig. 1-G is chromosome distribution of differentially

expressed genes. Compared to the parent A549 cells, approximately 2200 differentially expressed genes were upregulated, and 4300 differentially expressed genes were downregulated in cisplatin-resistant A549/DDP cells.

3.2. Function enrichment analysis

Fig. 2-A to F shows GO functional enrichment analysis, compared to the parent A549 cells, the cisplatin-resistant A549/DDP cells had different changes in molecular function categories, such as amide binding, protein binding, peptide binding, and enzyme activities. In addition, in the cellular component categories, there were cells and cell compositions with significant changes. Meanwhile, significant changes in biological process categories are mainly related to the cell cycle and metabolic processes.

The KEGG database is a database of cellular pathways. Using the classified entries of the KEGG pathway database, we can find the inter-relationship between differentially expressed genes and specific

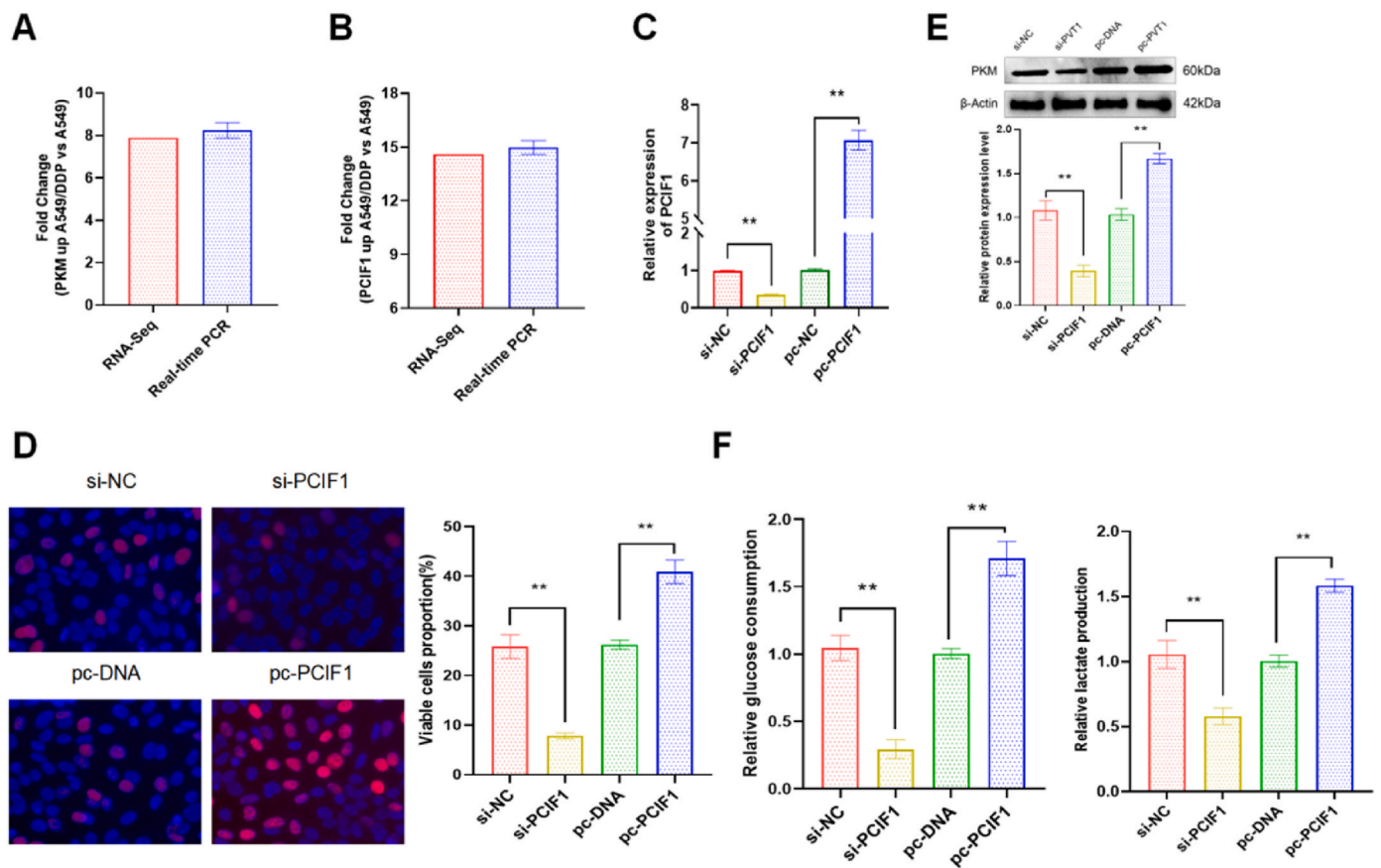


Fig. 4. Lnc-PCIF1 inhibited the glycolysis and cell viability of A549/DDP cells. RNA-Seq and qRT-PCR were used to detect the expression differences of (A) PCIF1 and (B) PKM genes. (C) The PCIF1 gene silencing or overexpression vectors were constructed and transfected, and the effect on PCIF1 gene expression was detected. (D) EdU method was used to detect cell proliferation activity. (E) The expression of PKM protein was detected by Western blot. (F) Intracellular glucose consumption and lactate accumulation were measured by Elisa. The experiments were repeated at least three times, and results were expressed as mean \pm S.D. *, $p < 0.05$; **, $p < 0.01$.

functional entries, thus promoting a greater understanding of the biological functions of transcription. As shown in Fig. 2-G and H, KEGG annotation results showed that compared to the parent A549 cells, the expression of genes related to the cell cycle pathway, DNA replication pathway, and cell metabolism pathway in cisplatin-resistant A549/DDP cells was significantly upregulated.

3.3. Construction of the ceRNA network for glycolysis regulation

GO and KEGG analyses and according to the enrichment score, it was inferred that abnormal changes in cell metabolism may be a reason for the occurrence of cisplatin resistance in A549/DDP cells. There are 200 differential genes involved in the regulation of metabolic abnormalities. Through further mining of KEGG data, it was found that there are 19 differential genes related to the regulation of glycolysis. According to the degree of difference in gene expression, the top six genes were selected—namely, *PKM*, *ALDOA*, *ENO1*, *ENO2*, *HK1*, and *PGAM1*. TargetScan and miRNA software were used to predict the miRNA targets and construct a ceRNA network map (Fig. 3).

3.4. Lnc-PCIF1 affects glycolysis and cell viability in A549/DDP cells

As shown in Fig. 4-A and 4-B, the experimental results of RNA-Seq were verified by qRT-PCR, and the results showed that there was no statistical difference between the two, indicating that the results of RNA-Seq data were very reliable. Compared with A549 cells, PKM and PCIF1 were increased by 7-fold and 14-fold in A549/DDP cells, respectively. As shown in Fig. 4-C and 4-D, the expression of PCIF1 in A549/DDP cells

transfected with si-PCIF1 was significantly decreased, and the cell proliferation activity was significantly decreased. The expression of PCIF1 in A549/DDP cells transfected with pc-PCIF1 was significantly increased, and the cell proliferation activity was significantly increased. As shown in Fig. 4-E, the expression level of PKM protein in A549/DDP cells transfected with si-PCIF1 was significantly decreased. The expression level of PKM protein in A549/DDP cells transfected with pc-PCIF1 was significantly increased. Finally, we examined the effect of PCIF1 on glucose consumption and lactate accumulation, and the results showed that glucose consumption and lactate accumulation were significantly reduced in A549/DDP cells transfected with si-PCIF1. The intracellular glucose consumption and lactate accumulation levels of A549/DDP cells transfected with pc-PCIF1 were significantly increased (Fig. 4-F).

3.5. Lnc-PCIF1 competed with PKM for miR-326 binding

As shown in Fig. 5-A, PCIF1 and miR-326 binding sites are predicted. Transfection of si-PCIF1 could significantly promote the expression level of miR-326, and transfection of pc-PCIF1 could significantly inhibit the expression level of miR-326 (Fig. 5-B). Similarly, transfection of miR-326 mimics in A549/DDP cells significantly inhibited the mRNA expression of PCIF-1, and transfection of miR-326 inhibitor significantly promoted the mRNA expression of PCIF-1 (Fig. 5-C). The results of dual-luciferase assay showed that the dual-luciferase activity was significantly decreased after co-transfection of miR-326 mimics and Wt-PCIF1 pmirGLO plasmids. The dual luciferase activity was significantly increased after co-transfection of miR-326 inhibitor and Wt-PCIF1 pmirGLO plasmids, but not changed in the Wt-PCIF1 pmirGLO

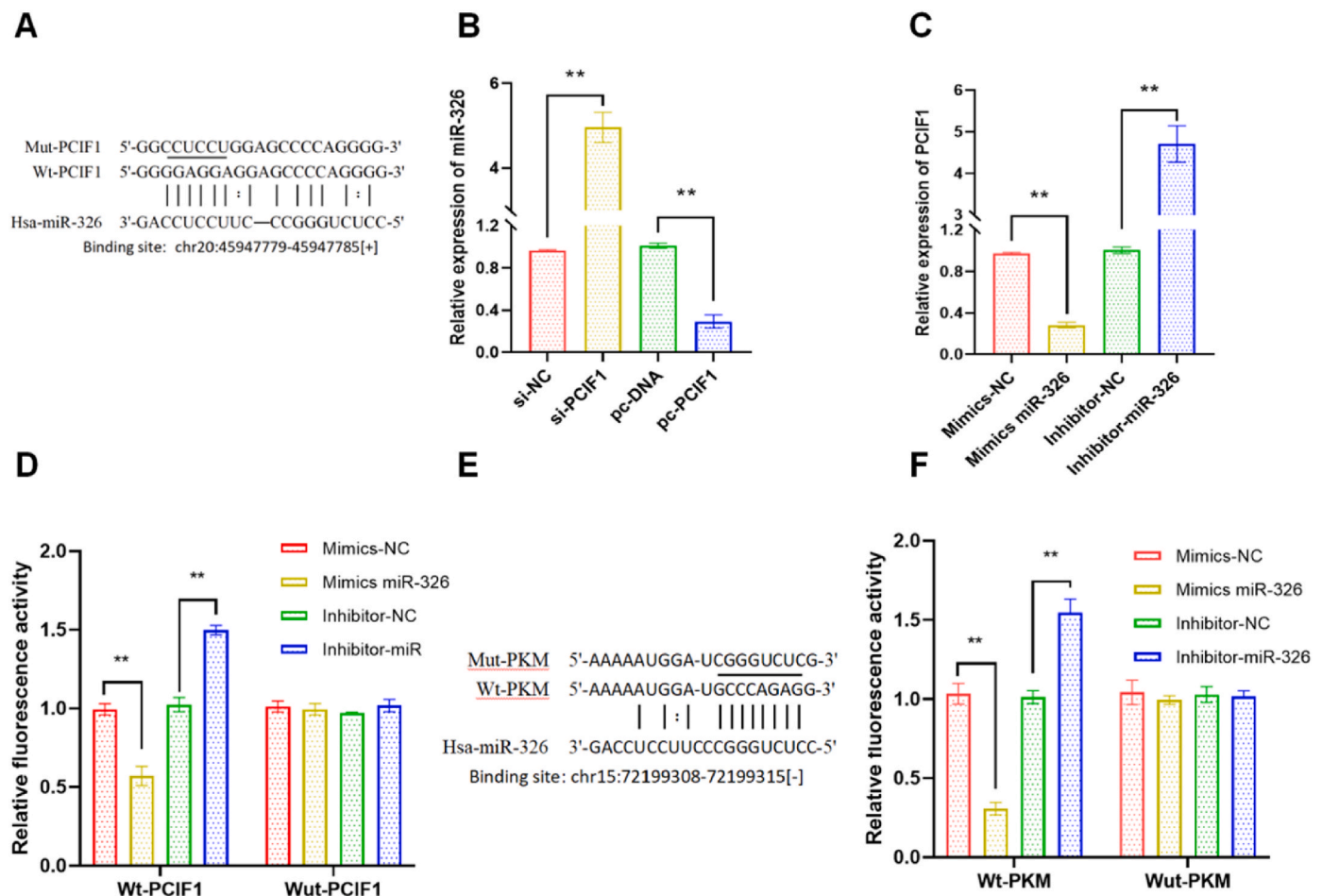


Fig. 5. Lnc-PCIF1 competed with PKM for miR-326 binding. (A) Prediction of Lnc-PCIF1 and miR-326 action sites. (B) Effect of PCIF1 on expression of miR-326. (C) Effect of miR-326 on PCIF1 expression. (D) Dual luciferase assay was used to detect the binding between PCIF1 and miR-326. (E) Prediction of PKM and miR-326 action sites. (F) Dual luciferase assay was used to detect the binding between PKM and miR-326. The experiments were repeated at least three times, and results were expressed as mean \pm S.D. *, $p < 0.05$; **, $p < 0.01$.

plasmids group (Fig. 5-D). As shown in Fig. 5-E, prediction of the binding sites of PKM and miR-326. Co-transfection of miR-326 mimics and Wt-PKM pmirGLO plasmids significantly decreased the dual luciferase activity, while co-transfection of miR-326 inhibitor and Wt-PKM pmirGLO plasmids significantly increased the dual luciferase activity. However, the activity values of dual luciferase did not change in the Mut-pKM pmirGLO plasmids group (Fig. 5-F).

3.6. Lnc-RNA PCIF1 inhibits the expression of PKM and promote cell apoptosis

As shown in Fig. 6-A, si-PCIF1+inhibitor-NC experimental group could inhibit the expression of PKM, and si-NC + miRNA-inhibitor experimental group could increase the expression of PKM. The expression level of PKM in the si-PCIF1+ miRNA-inhibitor group was similar. Similarly, glucose consumption and accumulated lactate levels were measured and the results showed that the si-PCIF1+inhibitor-NC group could inhibit glucose consumption and accumulated lactate levels compared with the si-NC + inhibitor-NC control group. The si-NC + miRNA-inhibitor experimental group could increase the glucose consumption and the cumulative level of lactate, while the si-PCIF1+ miRNA-inhibitor experimental group had similar glucose consumption and the cumulative level of lactate (Fig. 6-B). We use TUNEL and Western blot method to research the PCIF1 effects on apoptosis of A549/DDP cell. The results showed that si-PCIF1+inhibitor-NC group could promote the apoptosis of A549/DDP cells compared with si-NC +

inhibitor-NC control group. The si-NC + miRNA-inhibitor group could inhibit cell apoptosis, but the si-PCIF1+ miRNA-inhibitor group had no change in cell apoptosis (Fig. 6-C). Finally, in vivo experiments showed that si-PCIF1 could inhibit tumor growth and PKM expression in mice (Fig. 6-E and F).

4. Discussion

In the process of gene transcription, only 2 % of nucleic acid sequences are used to encode proteins, while the remaining 98 % of nucleic acid sequences cannot encode proteins [18]. RNA sequences that cannot encode proteins are called ncRNAs. In recent years, studies have found that such ncRNAs also have important biological functions, and they play an important regulatory role at the chromosome and transcriptional levels and in epigenetic modification [19–21]. In recent years, many studies have confirmed that miRNAs are involved in regulating tumor growth, differentiation, metastasis, proliferation, drug resistance, and other aspects [22–25]. However, with the deepening of research, new questions have also emerged, such as whether other factors can also affect the functional activity of miRNAs. Based on these questions, the ceRNA hypothesis was first proposed in 2011 [26], which revealed a new mechanism of RNA interaction—namely, a complementary pairing of ceRNAs and miRNAs, which affects the combination of miRNA and mRNA and ultimately realizes the regulation of mRNA expression. This is often closely related to the activation of oncogenes, the deterioration of tumors, and tumor metastasis [27]. Currently, the

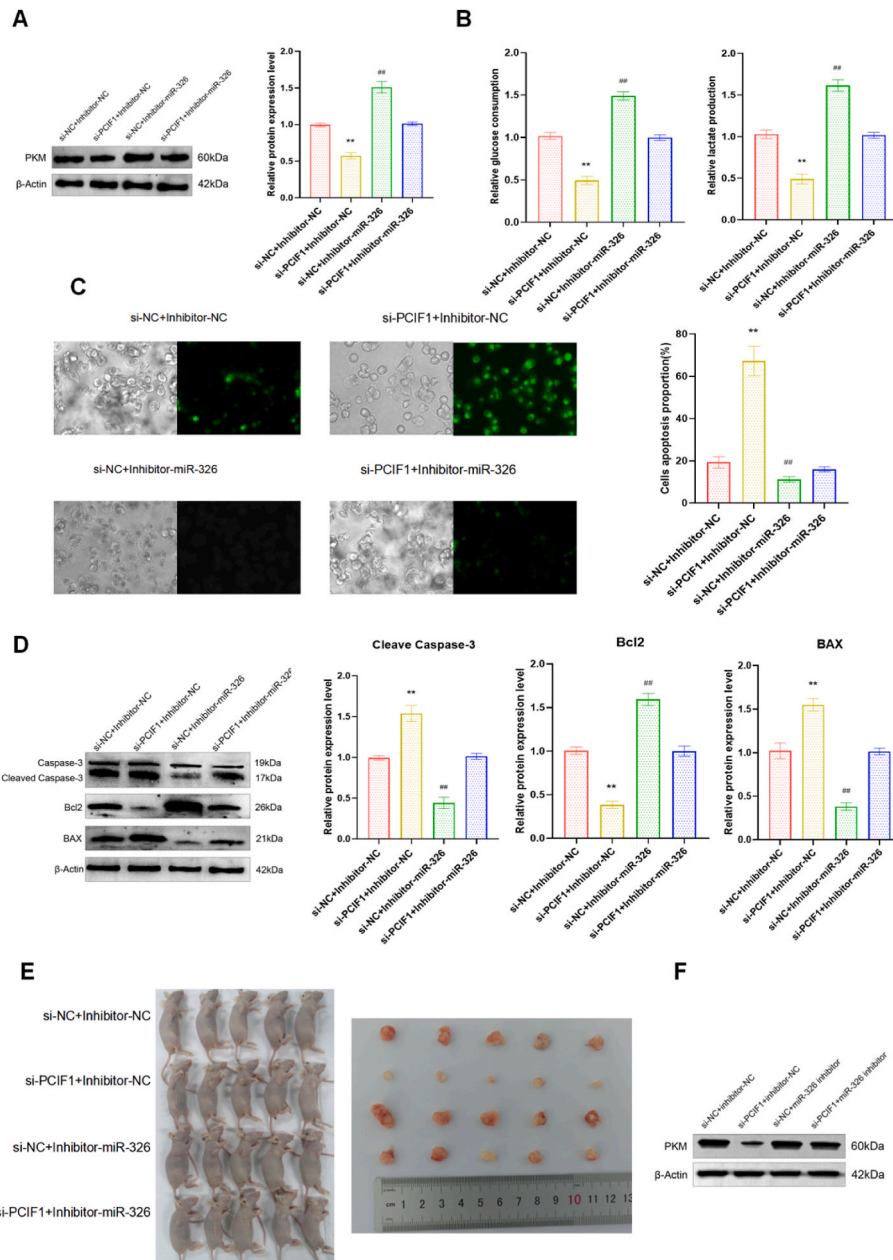


Fig. 6. Lnc-PCIF1 regulates glycolysis and apoptosis in A549/DDP cells. (A) The expression of PKM protein was detected by Western blot. (B) Intracellular glucose consumption and lactate accumulation were measured by Elisa. (C) Cell apoptosis was detected by TUNEL assay. (D) Cell apoptosis was detected by Western blot. (E) Tumor growth in tumor-bearing mice. (F) The expression of PKM protein in tumor tissues was detected by Western blot. The experiments were repeated at least three times, and results were expressed as mean ± S.D. * and # , $p < 0.05$; ** and ## , $p < 0.01$.

ceRNAs discovered mainly include circRNAs, lncRNAs, synthetic miRNAs, and viral miRNAs [28]. Studies have revealed a significant increase in the expression of lncRNA GLCC1 in colorectal cancer, leading to the promotion of glycolysis and subsequently enhancing cell survival and proliferation [29]. Studies have found that the expression of lncRNA HOTAIRM1 is increased in NSCLC, which can promote the level of glycolysis metabolism, the viability, migration and invasion of tumor cells [30].

The incidence and mortality rates of lung cancer have ranked it among the top three types of tumors worldwide for a long time. Non-small-cell lung cancer (NSCLC) is the most common type of lung cancer [31]. Most patients have lymph node or distant organ metastasis at the time of diagnosis [32]. A combination drug regimen based on platinum drugs is the first choice for the treatment of NSCLC, but with the increase in chemotherapy times, patients show resistance to platinum drugs,

which seriously affects the clinical efficacy of NSCLC treatment [33]. In recent years, metabolic reprogramming has been considered to be one of the 10 characteristics of tumor cells, in which glycometabolism reprogramming plays an important role, and glycometabolism reprogramming of tumor cells has received increasing attention in the research of tumor drug resistance mechanisms [34,35]. Currently, it has been found that several key enzymes of glucose metabolism are related to the drug resistance of tumor cells [36]. Among them, hexokinase (HK) catalyzes the first step of the glycolysis reaction, and it is a rate-limiting enzyme in the glycolysis pathway. Research shows that the application of HK-targeted small-molecule inhibitors combined with paclitaxel can significantly prolong the survival time of mice with NSCLC [37]. Pyruvate kinase (PK) is another rate-limiting enzyme in the glycolysis pathway that catalyzes the production of pyruvate and ATP. Studies have confirmed that the inhibition of PKM2 activity can reduce the

glycolysis level and ATP production level of tumor cells and enhance the sensitivity of cells to cisplatin drugs [38,39]. Lactic acid dehydrogenase (LDH) is a third key glycolysis-related enzyme able to convert pyruvate into lactic acid, inhibit the expression of LDH or reduce the enzyme activity, and improve the drug resistance of tumor cells to paclitaxel and trastuzumab [40,41].

In this study, the cisplatin-resistant A549/DDP cell line and its parent A549 cell line were selected as research objects. First, cisplatin chemotherapeutic drugs were administered to the two cell lines, and the results showed that the growth-inhibition effect of cisplatin on A549/DDP cells was significantly smaller than that on A549 cells. It was also found that the glucose consumption and lactic acid production of A549/DDP cells were greater than those of A549 cells. These results suggest that the drug resistance of A549/DDP cells might be related to abnormal glycolysis. Subsequently, we performed RNA-seq of A549/DDP and A549 cells, and then analyzed their differentially expressed genes at the gene and transcription levels. The results showed that A549/DDP cells had significant differences in gene expression and transcription level compared to A549 cells. In A549/DDP cells, approximately 4000 mRNAs were upregulated (the maximum upregulated factor was 23-fold), while approximately 5000 mRNAs were downregulated (the maximum downregulated factor was 138-fold). The enrichment analysis of GO terms and KEGG pathways for these different mRNAs showed that the genes involved in the cell metabolic pathway in A549/DDP cells were activated, and the enrichment ranked in the top 10 of the overall difference ranking. Further analysis of the changed metabolic pathways revealed that there were significant differences in 19 genes related to sugar metabolism, such as *ALDOA*, *ENO1*, *ENO2*, *HK1*, *PKM* and *PGAM1*.

We constructed a ceRNA network map using TargetScan, miRNA software, and the degree of difference in lncRNA expression. Combined with ceRNA network and RNA-Seq results, a regulatory complex, Lnc-PCIF1-miR-326-PKM, was selected. We confirmed that Lnc-PCIF1 could competitively combine with miR-326 to promote the expression of PKM by detecting changes in target genes by silencing or over-expressing genes in transfected cells, as well as dual-luciferase assay. In addition, we found that knockdown of Lnc-PCIF1 reduced glycolysis level and promoted apoptosis in A549/DDP cells. In this study, we verified that LncRNA PCIF1 has certain resistance to A549/DDP cells by in vivo and in vitro experiments. However, there are limitations in using only one cell line model and the lack of in vivo validation in other animal models, and we need to further verify the validity of these limitations in the future.

5. Conclusions

A549/DDP cell line as the NSCLC representative model bacterium, found the glycolytic pathway and related control gene increased significantly. Lnc PCIF1 as molecular sponge adsorption induced expression of PKM miR - 326 levels, promote the A549/DDP glycolysis and cisplatin resistance. As an early biomarker, Lnc PCIF1 affects the development of NSCLC. Early intervention targeting Lnc PCIF1 combined with other therapies can improve the therapeutic effect and prevent the occurrence of cisplatin resistance in NSCLC. More and deeper studies are needed to explore the differences of Lnc PCIF1 in other subtypes of NSCLC and whether this difference affects the efficacy of targeted Lnc-PCIF1 therapy, so as to provide theoretical basis for future clinical application.

Funding

This work was financially supported by Scientific Research Funding Project of Liaoning Provincial Department of Education (Grant No. LJKMZ20221785) and the National Natural Science Fund of China (Grant Nos. 82174254 and 81973735).

Ethical statement

This study was conducted at the School of Life Sciences and Health at Northeastern University in accordance with the Declaration of Helsinki and approved by the local Council of Governance (no. NEU-EC-2023A079S). Their care during research on animals follows ARRIVE guidelines and is conducted in accordance with the National Institutes of Health Guidelines for the Care and Use of Laboratory Animals (NIH Publication No. 8023, as revised in 1978).

CRediT authorship contribution statement

Wan Zhong: Data analysis. **Chun Wang:** Experimental design and funding support. **Ye Sun:** Experimental operation, funding support, data analysis and article writing.

Declaration of competing interest

There are no conflicts of interest to declare in this study.

Data availability

Data will be made available on request.

Acknowledgment

We thank LetPub (www.letpub.com) for its linguistic assistance during the preparation of this manuscript.

References

- [1] X. Zhang, W. Wang, W. Zhu, et al., Mechanisms and functions of long non-coding RNAs at multiple regulatory levels, *Int. J. Mol. Sci.* 20 (22) (2019) 5573–5601, <https://doi.org/10.3390/ijms20225573>.
- [2] T. Ravasi, H. Suzuki, K.C. Pang, et al., Experimental validation of the regulated expression of large numbers of non-coding RNAs from the mouse genome, *Genome Res.* 16 (1) (2006) 11–19, <https://doi.org/10.1101/gr.4200206>.
- [3] M. Guttman, I. Amit, M. Garber, et al., Chromatin signature reveals over a thousand highly conserved large non-coding RNAs in mammals, *Nature* 458 (7235) (2009) 223–227, <https://doi.org/10.1038/nature07672>.
- [4] H. Deng, J. Zhang, J. Shi, et al., Role of long non-coding RNA in tumor drug resistance, *Tumour Biol* 37 (9) (2016) 11623–11631, <https://doi.org/10.1007/s13277-016-5125-8>.
- [5] P. Ji, S. Diederichs, W. Wang, et al., MALAT-1, a novel noncoding RNA, and thymosin beta4 predict metastasis and survival in early-stage non-small cell lung cancer, *Oncogene* 22 (39) (2003) 8031–8041, <https://doi.org/10.1038/sj.onc.1206928>.
- [6] J.M. Silva-Fisher, H.X. Dang, N.M. White, et al., Long non-coding RNA RAMS11 promotes metastatic colorectal cancer progression, *Nat. Commun.* 11 (1) (2020) 2156, <https://doi.org/10.1038/s41467-020-15547-8>.
- [7] S. Gupta, R.F. Hashimoto, Dynamical analysis of a boolean network model of the oncogene role of lncRNA ANRIL and lncRNA UFC1 in non-small cell lung cancer, *Biomolecules* 12 (3) (2022) 420–438, <https://doi.org/10.3390/biom12030420>.
- [8] Y.T. Tan, J.F. Lin, T. Li, et al., LncRNA-mediated posttranslational modifications and reprogramming of energy metabolism in cancer, *Cancer Commun.* 41 (2) (2021) 109–120, <https://doi.org/10.1002/cac2.12108>.
- [9] L.A. Torre, R.L. Siegel, A. Jemal, Lung cancer statistics, *Adv. Exp. Med. Biol.* 893 (2016) 1–19, https://doi.org/10.1007/978-3-319-24223-1_1.
- [10] J.E. Chافت, A. Rimmer, W. Weder, et al., Evolution of systemic therapy for stages I-III non-metastatic non-small-cell lung cancer, *Nat. Rev. Clin. Oncol.* 18 (9) (2021) 547–557, <https://doi.org/10.1038/s41571-021-00501-4>.
- [11] S.K. Vinod, E. Hau, Radiotherapy treatment for lung cancer: current status and future directions, *Respirology* 2 (2020) 61–71, <https://doi.org/10.1111/resp.13870>.
- [12] Y. Tian, N. Wan, H. Zhang, et al., Chemoproteomic mapping of the glycolytic targetome in cancer cells, *Nat. Chem. Biol.* 19 (12) (2023) 1480–1491.
- [13] F. Paredes, H.C. Williams, A. San Martin, Metabolic adaptation in hypoxia and cancer, *Cancer Lett.* 502 (2021) 133–142.
- [14] M. Vahabi, A. Comandatore, M.A. Franczak, et al., Role of exosomes in transferring chemoresistance through modulation of cancer glycolytic cell metabolism, *Cytokine Growth Factor Rev* 73 (2023) 163–172.
- [15] K. Zahra, T. Dey, Ashish, et al., Pyruvate kinase M2 and cancer: the role of PKM2 in promoting tumorigenesis, *Front. Oncol.* 10 (2020) 159.
- [16] L. Traxler, J.R. Herdy, D. Stefanoni, et al., Warburg-like metabolic transformation underlies neuronal degeneration in sporadic Alzheimer's disease, *Cell Metab* 34 (9) (2022) 1248–1263.

- [17] M. Luo, Y. Luo, N. Mao, et al., Cancer-associated fibroblasts accelerate malignant progression of non-small cell lung cancer via connexin 43-formed unidirectional gap junctional intercellular communication, *Cell. Physiol. Biochem.* 51 (1) (2018) 315–336.
- [18] P.E. Saw, X. Xu, J. Chen, et al., Non-coding RNAs: the new central dogma of cancer biology, *Sci. China Life Sci.* 64 (1) (2021) 22–50, <https://doi.org/10.1007/s11427-020-1700-9>.
- [19] J. Xu, J. Bai, J. Xiao, Computationally modeling ncRNA-ncRNA crosstalk, *Adv. Exp. Med. Biol.* 1094 (2018) 77–86, https://doi.org/10.1007/978-981-13-0719-5_8.
- [20] J. Wang, S. Zhu, N. Meng, et al., ncRNA-encoded peptides or proteins and cancer, *Mol. Ther.* 27 (10) (2019) 1718–1725, <https://doi.org/10.1016/j.ymthe>.
- [21] F. Bocci, M.K. Jolly, H. Levine, et al., Quantitative characteristic of ncRNA regulation in gene regulatory networks, *Methods Mol. Biol.* 1912 (2019) 341–366, https://doi.org/10.1007/978-1-4939-8982-9_14.
- [22] E. Anastasiadou, L.S. Jacob, F.J. Slack, Non-coding RNA networks in cancer, *Nat. Rev. Cancer* 18 (1) (2018) 5–18, <https://doi.org/10.1038/nrc.2017.99>.
- [23] J. Zhang, A. Zhang, Y. Wang, et al., New insights into the roles of ncRNA in the STAT3 pathway, *Future Oncol.* 8 (6) (2012) 723–730, <https://doi.org/10.2217/fon.12.52>.
- [24] Y. Wang, Y. Wang, Z. Qin, et al., The role of non-coding RNAs in ABC transporters regulation and their clinical implications of multidrug resistance in cancer, *Expert Opin Drug Metab Toxicol* 17 (3) (2021) 291–306, <https://doi.org/10.1080/17425255.2021.1887139>.
- [25] B. Chen, M.P. Dragomir, C. Yang, et al., Targeting non-coding RNAs to overcome cancer therapy resistance, *Signal Transduct Target Ther* 7 (1) (2022) 121, <https://doi.org/10.1038/s41392-022-00975-3>.
- [26] X. Qi, D.H. Zhang, N. Wu, et al., ceRNA in cancer: possible functions and clinical implications, *J. Med. Genet.* 52 (10) (2015) 710–718, <https://doi.org/10.1136/jmedgenet-2015-103334>.
- [27] E.A. Braga, M.V. Fridman, A.A. Moscovtsev, et al., LncRNAs in ovarian cancer progression, metastasis, and main pathways: ceRNA and alternative mechanisms, *Int. J. Mol. Sci.* 21 (22) (2020) 8855, <https://doi.org/10.3390/ijms21228855>.
- [28] J. Tang, T. Yan, Y. Bao, et al., LncRNA GLCC1 promotes colorectal carcinogenesis and glucose metabolism by stabilizing c-Myc, *Nat. Commun.* 10 (1) (2019) 3499.
- [29] D. Chen, Y. Li, Y. Wang, et al., LncRNA HOTAIRM1 knockdown inhibits cell glycolysis metabolism and tumor progression by miR-498/ABCE1 axis in non-small cell lung cancer, *Genes Genomics* 43 (2) (2021) 183–194.
- [30] J. Long, Y. Bai, X. Yang, et al., Construction and comprehensive analysis of a ceRNA network to reveal potential prognostic biomarkers for hepatocellular carcinoma, *Cancer Cell Int.* 19 (2019) 90, <https://doi.org/10.1186/s12935-019-0817-y>.
- [31] R.L. Siegel, K.D. Miller, A. Jemal, Cancer statistics, 2019, *CA Cancer J Clin* 69 (1) (2019) 7–34, <https://doi.org/10.3322/caac.21551>.
- [32] L. Yin, X. Liu, X. Shao, et al., The role of exosomes in lung cancer metastasis and clinical applications: an updated review, *J. Transl. Med.* 19 (1) (2021) 312, <https://doi.org/10.1186/s12967-021-02985-1>.
- [33] Z.F. Lim, P.C. Ma, Emerging insights of tumor heterogeneity and drug resistance mechanisms in lung cancer targeted therapy, *J. Hematol. Oncol.* 12 (1) (2019) 134, <https://doi.org/10.1186/s13045-019-0818-2>.
- [34] M. Zdravlević, A. Brand, L. Di Ianni, et al., Double genetic disruption of lactate dehydrogenases A and B is required to ablate the "Warburg effect" restricting tumor growth to oxidative metabolism, *J. Biol. Chem.* 293 (41) (2018) 15947–15961, <https://doi.org/10.1074/jbc.RA118.004180>.
- [35] J. Jin, S. Qiu, P. Wang, et al., Cardamonin inhibits breast cancer growth by repressing HIF-1 α -dependent metabolic reprogramming, *J. Exp. Clin. Cancer Res.* 38 (1) (2019) 377, <https://doi.org/10.1186/s13046-019-1351-4>.
- [36] J. Zuo, J. Tang, M. Lu, et al., Glycolysis rate-limiting enzymes: novel potential regulators of rheumatoid arthritis pathogenesis, *Front. Immunol.* 12 (2021) 779787, <https://doi.org/10.3389/fimmu.2021.779787>.
- [37] D. Palmieri, D. Fitzgerald, S.M. Shreeve, et al., Analyses of resected human brain metastases of breast cancer reveal the association between up-regulation of hexokinase 2 and poor prognosis, *Mol. Cancer Res.* 7 (9) (2009) 1438–1445, <https://doi.org/10.1158/1541-7786>.
- [38] T.L. Dayton, T. Jacks, M.G. Vander Heiden, PKM2, cancer metabolism, and the road ahead, *EMBO Rep.* 17 (12) (2016) 1721–1730, <https://doi.org/10.15252/embr.201643300>.
- [39] H. Chang, Q. Xu, J. Li, et al., Lactate secreted by PKM2 upregulation promotes Galectin-9-mediated immunosuppression via inhibiting NF- κ B pathway in HNSCC, *Cell Death Dis.* 12 (8) (2021) 725, <https://doi.org/10.1038/s41419-021-03990-4>.
- [40] F. Madani, S.S. Esnaashari, M.C. Bergonzi, et al., Paclitaxel/methotrexate co-loaded PLGA nanoparticles in glioblastoma treatment: formulation development and in vitro antitumor activity evaluation, *Life Sci.* 256 (2020) 117943, <https://doi.org/10.1016/j.lfs.2020.117943>.
- [41] Y. Zhao, H. Liu, Z. Liu, et al., Overcoming trastuzumab resistance in breast cancer by targeting dysregulated glucose metabolism, *Cancer Res.* 71 (13) (2011) 4585–4597, <https://doi.org/10.1158/0008-5472.CAN-11-0127>.